

REU 2004 Summer Program

Modeling Changes in  
Brain Pressures, Volumes, and  
Cerebral Capillary Fluid Exchange:  
Hydrocephalus

Student's Name: Sean Anderson  
Advisor: Prof. A. Linninger

Laboratory for Product and Process Design  
University of Illinois at Chicago  
LPPD-Project Report: 08/05/2004

## Table of Contents

Abstract .....	3
Introduction .....	4
Methods .....	5
Pressure-Volume Compartmental Model: Background .....	5
Pressure-Volume Compartmental Model: Pressure Theory .....	5
Pressure-Volume Compartmental Model: Volume Theory .....	7
Cerebral Capillary Fluid Exchange Model .....	9
Results .....	10
Compartmental Model: Pressures .....	10
Compartmental Model: Volumes .....	13
Cerebral Capillary Fluid Exchange Model .....	17
Discussion .....	20
Compartmental Model: Pressures .....	20
Compartmental Model: Volumes .....	20
Cerebral Capillary Fluid Exchange Model .....	21
Conclusion .....	23
References .....	24
Appendix A .....	25
Appendix B .....	26
Appendix C .....	28
Appendix D .....	29

## **Abstract**

A comprehensive compartmental model of the human brain pressure and volume changes was developed over the summer of 2004 in the Laboratory for Product and Process Design (LPPD) at the University of Illinois at Chicago under the direction of Professor Andreas Linninger in order to study hydrocephalus and its effect on brain hemodynamics. Moreover, a cerebral capillary fluid exchange model was also developed to study the pressure gradients involved in water transport across the blood-brain barrier in cerebral capillaries. The model was developed conceptually and simulated using PLECS in Simulink. Further analysis was completed in MATLAB. We found physiologically sound results that describe the brain pressure and volume changes during normal conditions and during hydrocephalus. The arterial pressure remains constant. The capillary pressure decreases. Meanwhile, the intracranial pressure (ICP), venous pressure, and Sagittal Sinus pressure all increase. From this, the arterial volume remains relatively constant. The venous volume and the brain parenchyma volume decrease significantly, as expected. Because of cerebrospinal fluid (CSF) buildup, the ventricular system expands and increases in volume. In the cerebral capillary, it was found that a mechanism exists to reverse the volume flux and drive extracellular fluid into the cerebral capillaries. This is an exciting finding that can lead to improved research in the future.

**Key words:** *Hydrocephalus, Intracranial Pressure, Cerebrospinal Fluid, Extracellular Fluid, Brain Parenchyma, Ventricular System*

## Introduction

Hydrocephalus is a disease which affects thousands of people annually in the United States alone (Linninger 2004). The disease is debilitating and can cause serious injury, even death in extreme circumstances. The current treatment for the disease is inconsistent and inadequate (Roycewicz 2004). A better treatment is needed and must be developed. In order to develop an enhanced treatment, however, a greater understanding of the disease and its effects on the brain is necessary.

At the onset of hydrocephalus, cerebrospinal fluid (CSF), which normally acts to cushion the brain from impact, builds up in the ventricular space, where it is produced. It is believed that the failure of the Sagittal Sinus—the location of CSF absorption into the venous system—is the cause for this buildup (Linninger 2004). As the ventricular system expands to compensate for this buildup in CSF, the brain parenchyma tissue is compacted. Normal functions are still available, however. Thus, brain cells do not die when the tissue is compressed. What happens, though, remains elusive.

Winston (1991) hypothesized that the fluid surrounding the brain cells, known as extracellular fluid, drains from the tissue volume to the ventricular system. However, we believe that this is not true. If this were in fact the case, then the ventricular space would not expand as a function of CSF production (Linninger 2004). Rather, it would expand as a function of the extracellular fluid drainage in addition to CSF production.

We hypothesize that the extracellular fluid is absorbed in the cerebral capillaries and carried away from the brain system. This leaves room for the ventricular system to expand and the brain tissue space to be compressed without loss of function or death of brain cells.

In 1976, Hakim began a physics approach to medical research with a landmark article. He studied hydrocephalus in relation to brain hemodynamics research. He found that the intracranial pressure (ICP) is the pressure of interest when studying hydrocephalus. The ICP increases when hydrocephalus occurs (Hakim 1976, Linninger 2004). The ICP controls brain volume changes and cerebral capillary fluid exchange.

We have proposed a model that examines the pressure-volume dynamics of the brain. Furthermore, we have also developed a model of the cerebral capillary fluid exchange. It is the goal of this research to determine whether a mechanism exists through which the extracellular fluid in the brain parenchyma can be absorbed by the cerebral capillaries.

In this paper, the theory and methods by which the results were obtained will be presented first. The theory behind the pressure-volume compartmental model and the capillary fluid exchange model will be derived and explained. Second, the results of the simulations at different levels of hydrocephalus will be displayed and discussed. An interpretation of these results pertaining to their physical relevance will follow. Finally, the paper will close with a conclusion and suggestions for future work. In the back of this report, there are appendices that include the Simulink, PLECS, and MATLAB codes, a table of all physical constants and properties used during the course of this project, and a note on the development of the pressure equations of the circuit analogy.

## Methods

### *Pressure-Volume Compartmental Model: Background*

The Pressure-Volume Compartmental model is composed of interacting pressures and volumes in the brain. The four compartments include the arterial volume, the venous volume, the brain parenchyma volume, and the CSF ventricular volume. The arterial volume is the blood and oxygen supply to the brain system via arteries. The venous volume is the blood and other constituent matter leaving the brain system and being recycled to the heart. The brain parenchyma is the actual brain tissue (nerves and extracellular fluid) and the cerebral capillary system. Finally, the CSF ventricular volume includes the volume of CSF in the system and the space that is occupied by the ventricular system as a whole (Ursino 1988). This model is broken down and visualized below.

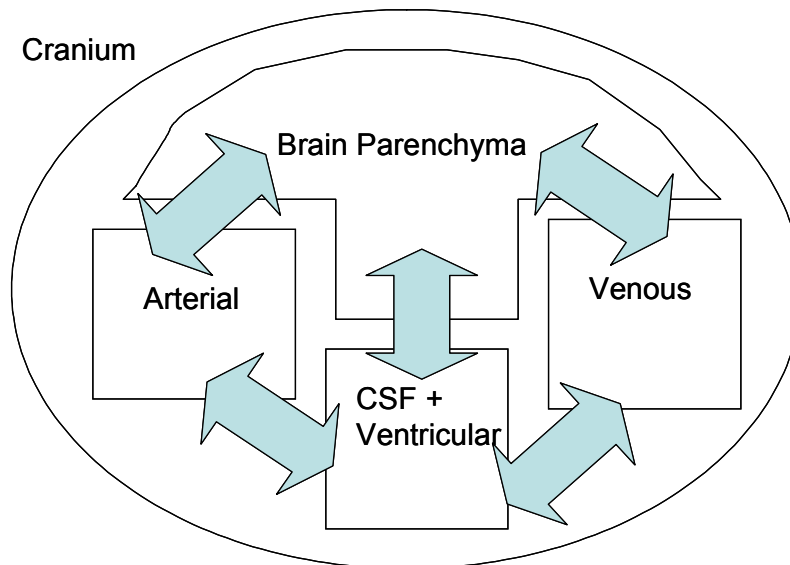


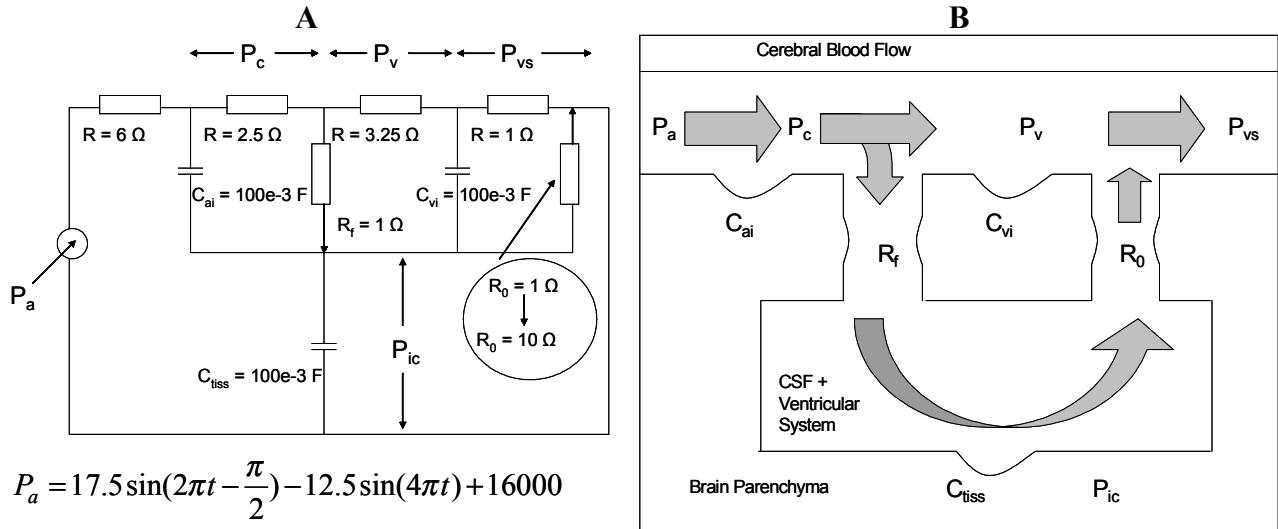
**Figure 1: Concept of compartmental model showing inter-relationships of pressures and volumes in the human brain**

### *Pressure-Volume Compartmental Model: Pressure Theory*

In order to obtain the pressures in the compartmental model, a simulation of a circuit analog to the brain system (Ursino 1988, 1997) was completed in the PLECS package of Simulink (Appendix A). To start, two sine waves were subtracted from each other to acquire the desired pressure waveform shown on the left in Figure 3(Xenos 2004):

$$P_a = 17.5 \sin(2\pi t - \frac{\pi}{2}) - 12.5 \sin(4\pi t) + 16000 \quad (1)$$

Then, with the circuit depicted below, the simulation gave an output of the pressures; more commonly known as the voltages in this circuit analog. The circuit is derived from a flow chart of the cerebral fluid system, which is also shown below (Ursino 1997).



$$P_a = 17.5 \sin(2\pi t - \frac{\pi}{2}) - 12.5 \sin(4\pi t) + 16000$$

Figure 2: (A) Circuit analog of cerebral system (Ursino 1997).

(B) Concept of cerebral system from which the circuit was derived (Ursino 1997).

After an evaluation of the capacitor equations, (7)-(9), the capacitors in the circuit were assumed to be small and constant. These capacitors were used to tune the time delay of the pressure waves. Based on literature data (Ursino 1988), the pressures were further tuned by the resistance parameters (Appendix C). These parameters were tuned until the pressure waveforms matched the values found in Figure 3. While the resistance parameters hold no physiological value, the pressure waveforms they produce follow data well (Ursino 1988, Linninger 2004). Furthermore, hydrocephalus was simulated by increasing the resistance at the absorption site of CSF. The failure of the Sagittal Sinus, which is where the CSF is absorbed into the venous system, is thought to be the cause of most cases of hydrocephalus (Linninger 2004).

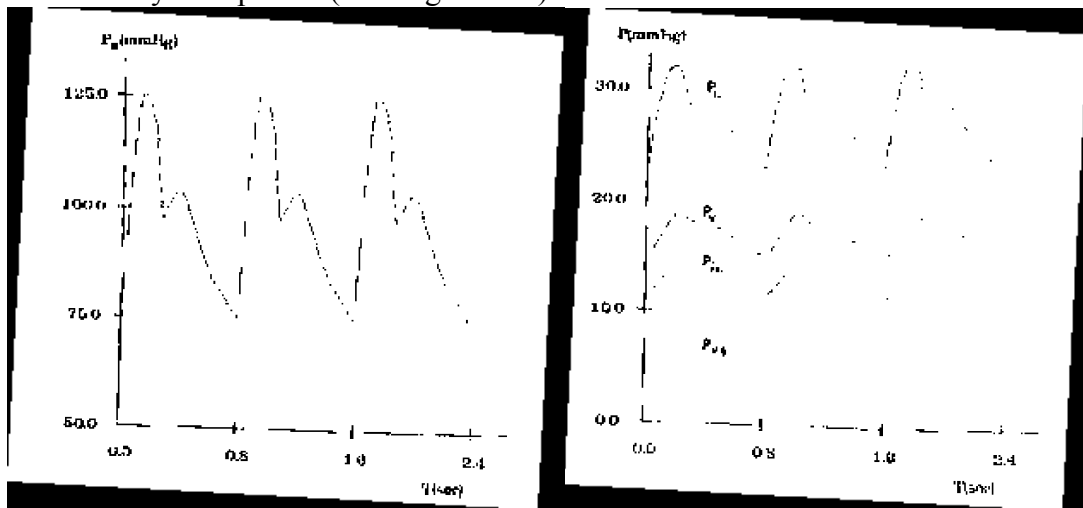


Figure 3: Resistance parameters were tuned to generate pressure waves matching these (Ursino 1988)

In Figure 2(B), the blood supply from the heart to the brain is shown by the cerebral blood flow (horizontal pipe). The blood flows from the artery, to the capillaries, and then to the veins. Meanwhile, the two vertical pipes and the tank represent the ventricular system. CSF is produced at the site of the vertical pipe leading downward ( $R_f$ ). This production site is referred to as the Choroid Plexus. The CSF then flows around the brain in the Subarachnoidal Space and is absorbed into the venous system at the Sagittal Sinus, portrayed by the pipe going upward ( $R_0$ ). The capacitors are called the compliances of the tissues in this analogy. They describe the elasticity of the various compartments: arterial, venous, and parenchyma.

*Pressure-Volume Compartmental Model: Volume Theory*

Using the pressures from above, the different compartment volumes of the brain can be obtained (Ursino 1988, 1991, 1997). First, we begin with an overall mass balance of the four interacting compartments of the brain (Monro-Kellie doctrine):

$$\frac{dV_a}{dt} + \frac{dV_v}{dt} + \frac{dV_{tiss}}{dt} + \frac{dV_{CSF}}{dt} = 0 \quad (2)$$

where  $a$  denotes arterial system,  $v$  denotes venous system,  $tiss$  denotes brain parenchyma, and  $CSF$  denotes the ventricular system (Winston 1991, Ursino 1988). This relation makes perfect physiological sense. The overall change in volume of the brain must be zero. This means that the brain volume is constant. While different departments may grow in size (i.e. ventricular system), it is only at the expense of other components (i.e. arterial, venous, and brain parenchyma).

Each volume is described by separate equations describing human intracranial dynamics (Ursino 1988):

$$\frac{dV_a}{dt} = C_{ai} \frac{d}{dt}(P_a - P_{ic}) \quad (3)$$

$$\frac{dV_v}{dt} = C_{vi} \frac{d}{dt}(P_v - P_{ic}) \quad (4)$$

$$\frac{dV_{tiss}}{dt} = -C_{tiss} \frac{dP_{ic}}{dt} \quad (5)$$

$$\frac{dV_{CSF}}{dt} = \frac{P_c - P_{ic}}{R_f} - \frac{P_{ic} - P_{vs}}{R_0} \quad (6)$$

where the  $C$ 's are compliances of the certain compartments which are described by the circuit analog Figure 2(A) and compared to literature values (Appendix C).

The expressions for the compliances based on circuit analysis are given below (Ursino 1988):

$$C_{ai} = \frac{1}{K_a (P_a - P_{ic})} \quad (7)$$

$$C_{vi} = \frac{1}{K_v (P_v - P_{ic} - P_{vl})} \quad (8)$$

$$C_{tiss} = \frac{1}{K_E \left[ P_{ic} + \left( \frac{P_{ic}}{P_{01}} \right)^2 \right]} \quad (9)$$

where the  $K$ 's, and constant  $P$ 's are defined in Appendix C (Ursino 1988).

Combining equation (3) with (7) gives an expression for the arterial volume in terms of constants and pressures:

$$\frac{dV_a}{dt} = \frac{1}{K_a} \frac{d(P_a - P_{ic})}{(P_a - P_{ic})} \quad (10)$$

After some mathematical manipulations, we have:

$$dV_a = \frac{1}{K_a} \frac{d(P_a - P_{ic})}{(P_a - P_{ic})} \quad (11)$$

Upon integration, we obtain an expression for the arterial compartment volume:

$$V_a = \frac{1}{K_a} \ln(P_a - P_{ic}) + V_{ai} \quad (12)$$

In a similar fashion, we get the venous and tissue volumes as shown here:

$$V_v = \frac{1}{K_v} \ln(P_v - P_{ic} - P_{vl}) + V_{vi} \quad (13)$$

$$V_{tiss} = -\frac{P_{01}^2 \ln\left(P_{ic}^2 + P_{01}^2 \frac{P_{ic}}{P_{01}}\right)}{K_E (2P_{ic} + P_{01}^2)} + V_{tissi} \quad (14)$$

The last volume, the ventricular system, is found by utilizing the Monro-Kellie doctrine (Winston 1991, Ursino 1988). Solving for  $\frac{dV_{CSF}}{dt}$  we have:

$$\frac{dV_{CSF}}{dt} = -\frac{dV_a}{dt} - \frac{dV_v}{dt} - \frac{dV_{tiss}}{dt} \quad (15)$$

Again, with some mathematical manipulations, we have:

$$dV_{CSF} = -dV_a - dV_v - dV_{tiss} \quad (16)$$

Upon integration, we are left with  $V_{CSF}$  in terms of the other volumes:

$$V_{CSF} = -(V_a - V_{ai}) - (V_v - V_{vi}) - (V_{tiss} - V_{tissi}) + V_{CSFi} \quad (17)$$

These volumes were subsequently evaluated using MATLAB (Appendix B). Values for the initial volumes were extracted from literature (Appendix C).

### *Cerebral Capillary Fluid Exchange Model*

The second part of this project was to model the diffusion of water in the cerebral capillaries (Paulson 1977). Here, we have the extracellular fluid flux across a brain capillary (Fournier 1998):

$$J = L_p S ((P_c - P_{ic}) - (\Pi_c - \Pi_{ic})) \quad (18)$$

The constants and osmotic pressures in this equation can be found in Table 1 (Appendix C). The  $\Pi$ 's are the capillary and intracranial osmotic pressures, respectively. These pressures are normally smaller than the main pressures (MacLeod 2004). In this model, the osmotic pressure was assumed to remain constant, as no difference in solute concentration was imposed on the system.

By using the pressure waves generated from the circuit under normal and hydrocephalus conditions, the behavior of the fluid flux was found. Winston (1991) has claimed that when the parenchyma volume is reduced during hydrocephalus, the extracellular fluid drains into the ventricular system. On the other hand, we have proposed that the extracellular fluid drains into the cerebral capillaries. By studying the volume flux at the cerebral capillary, it is possible to determine whether the normal flux pattern—fluid diffusing outward—can be reversed when the system is stressed from the conditions of hydrocephalus.

## Results

### *Compartmental Model: Pressures*

The pressure waves were evaluated from a circuit analogy of brain dynamics. The five pressure waves for the first simulation are shown in Figure 4. In the first simulation, the absorption resistance at the Sagittal Sinus was assigned a value of  $10\Omega$  in the hydrocephalus regime. The value was arbitrarily chosen, yet it is known that the absorption resistance in patients with hydrocephalus increases 10-fold (Linninger 2004).

These pressure waves follow the pulsatile motion of the heart beat. Because of the different locations in the cerebral system, the waves experience changes in magnitude and phase (Danzinger 2003). The arterial pressure ( $P_a$ ) is the largest and closest to the heart source. The next largest wave is the capillary pressure ( $P_c$ ). As the wave propagates through the brain, it traverses from the artery to the capillary. As you can see, the waveform is significantly muted and dampened (Zagzoule 1986). The elasticity of the walls of the arteries absorbs the kinetic energy of the pressure wave and reduces its amplitude (Danzinger 2003). From the capillary, the blood then travels to the venous system, where the waveform ( $P_v$ ) is further dampened. Here, the blood exits the cerebral system and returns to the heart and lungs for recycling (Zagzoule 1986).

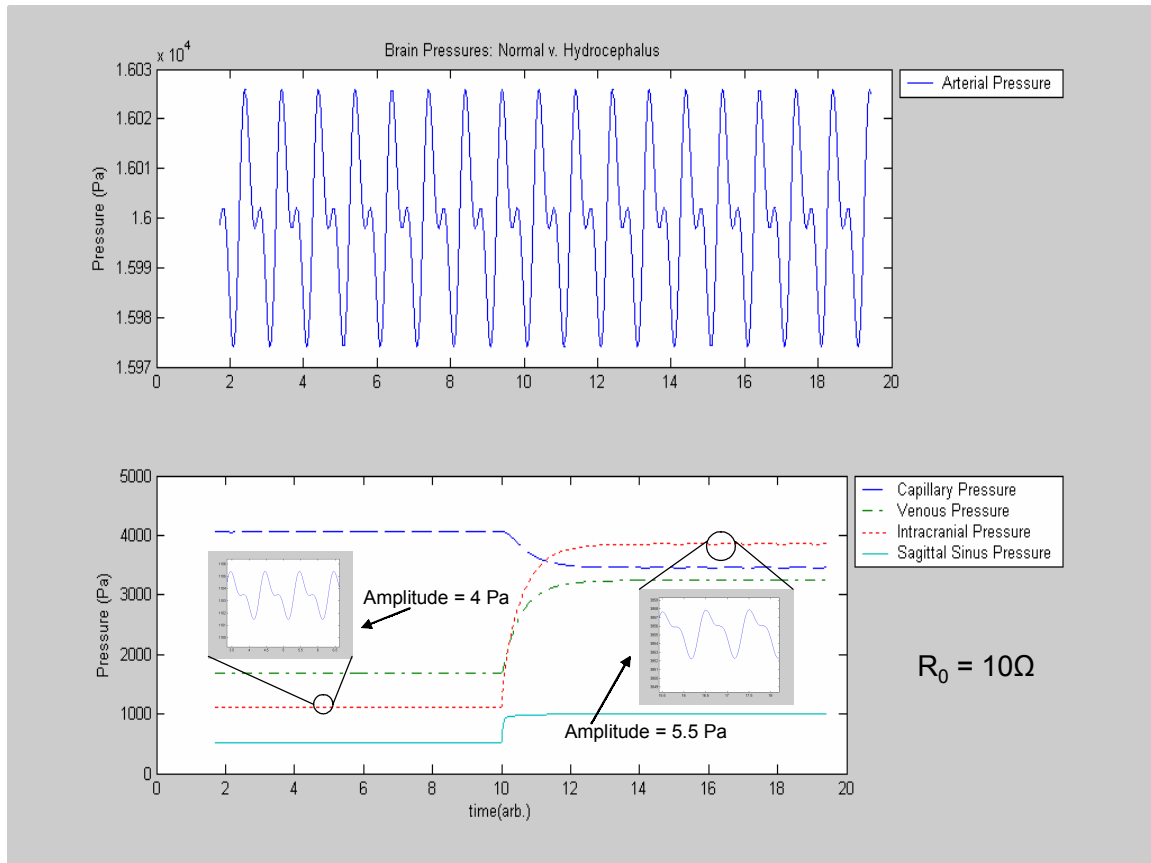


**Figure 4: Pressure waves in brain during normal and hydrocephalus conditions.**

The pressure waves from the cerebral blood flow are propagated further in the brain system through the cerebrospinal fluid (CSF). CSF is produced in the Choroid Plexus where the pressure transmits itself from the arterial and capillary system to the ventricular system (Danzinger 2003). However, pressures here are less than that of the venous system (Ursino 1988). The intracranial pressure (ICP or  $P_{ic}$ ) is the next largest waveform after the venous waveform. This, of course, is under normal circumstances, and not under hydrocephalus conditions. The smallest waveform in Figure 4 is the pressure at the CSF absorption site at the Sagittal Sinus ( $P_{vs}$ ). Under normal conditions, this pressure is small because it is at the end of the line in a series of propagations through the system. When the wave reaches this point, it is severely dampened. The pulsations are muted and amplitude is small.

When hydrocephalus occurs, the order of the pressure waves changes—depending on the value of the absorption resistance. To reiterate, hydrocephalus is simulated by increasing the absorption resistance of CSF exiting the ventricular system and entering the venous system for disposal. In Figure 4, the arterial pressure wave is unaffected by hydrocephalus. This makes physiological sense since it is not affected by the CSF blockage; rather, it is dependent on the heart. On the other hand, the other pressures are severely affected by the change from normal to hydrocephalus conditions. The venous pressure goes up along with the intracranial pressure. However, the ICP increases dramatically, as expected from experimental data. Furthermore, the amplitude of the oscillations of the ICP wave also increases, following previous simulations and experiments (Linninger 2004). Most interesting, however, is the behavior of the capillary pressure. The capillary pressure decreases. When steady state is reached under the hydrocephalus regime, the capillary pressure is less than the intracranial pressure. This affects the flux equation, (18), but an analysis of this is discussed later.

Finally, the pressure at the Sagittal Sinus increases slightly. The difference between the ICP and Sagittal Sinus pressure follows previous experiments performed on dogs (Linninger 2004). Under normal conditions, the difference is about 600 Pa. With hydrocephalus, the difference increases to about 3000 Pa. This follows the behavior of dogs with chronic hydrocephalus (Linninger 2004).

A second simulation was run at a lower absorption resistance level,  $7\Omega$ . This was done to study the volume changes and flux changes when the order of the pressure waves is different during the hydrocephalus regime. In Figure 5, the capillary pressure is now slightly larger than the ICP. Nonetheless, the amplitude change of the ICP and Sagittal Sinus between normal and hydrocephalus remain the same. The difference between the ICP and Sagittal Sinus pressure is now 2500 Pa, which is still in the range of chronic hydrocephalus (Linninger 2004).

In the third simulation, an absorption resistance of  $5\Omega$  was implemented. Now, the capillary pressure is significantly above the ICP. The amplitude change in the oscillations for ICP and  $P_{vs}$  remains, however, and is still consistent with previous studies (Linninger 2004). Furthermore, the difference between the ICP and Sagittal Sinus pressure drops to about 2000 Pa, which is a less severe case of hydrocephalus (Linninger 2004).

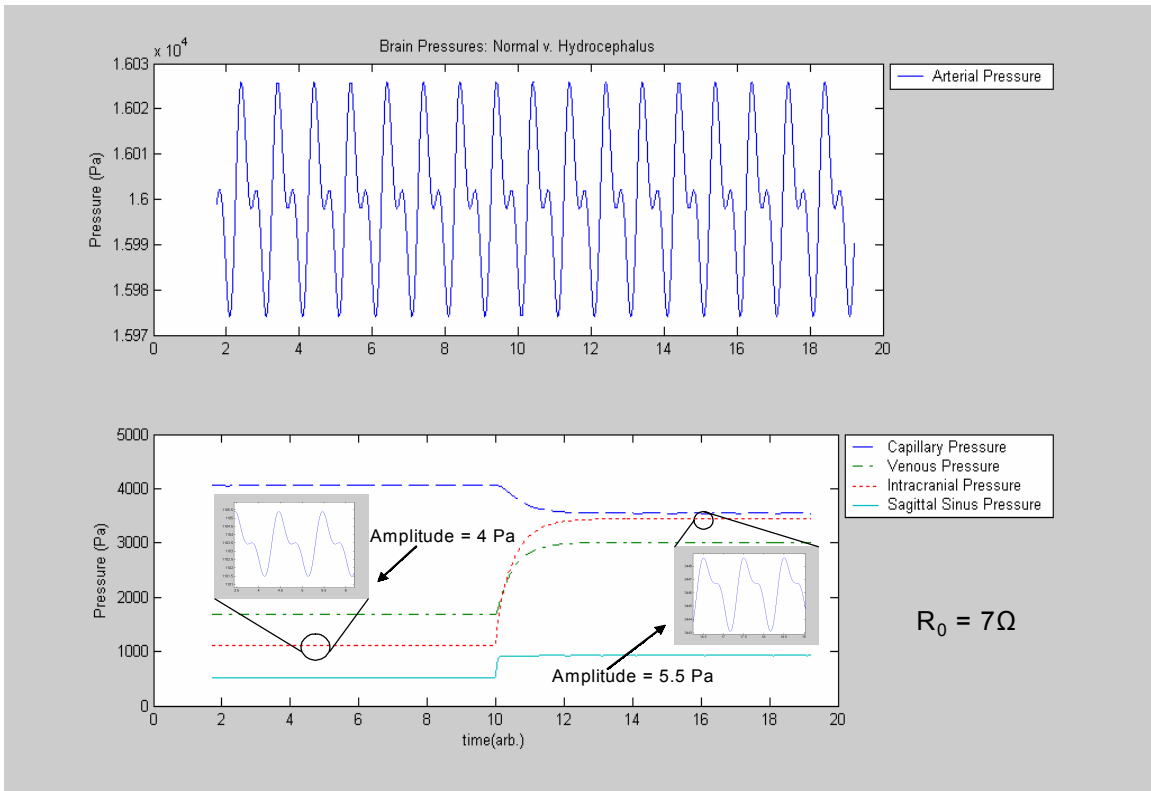


**Figure 5: Simulation run at slightly lower resistance level. Here, capillary pressure is larger than ICP in the hydrocephalus regime.**

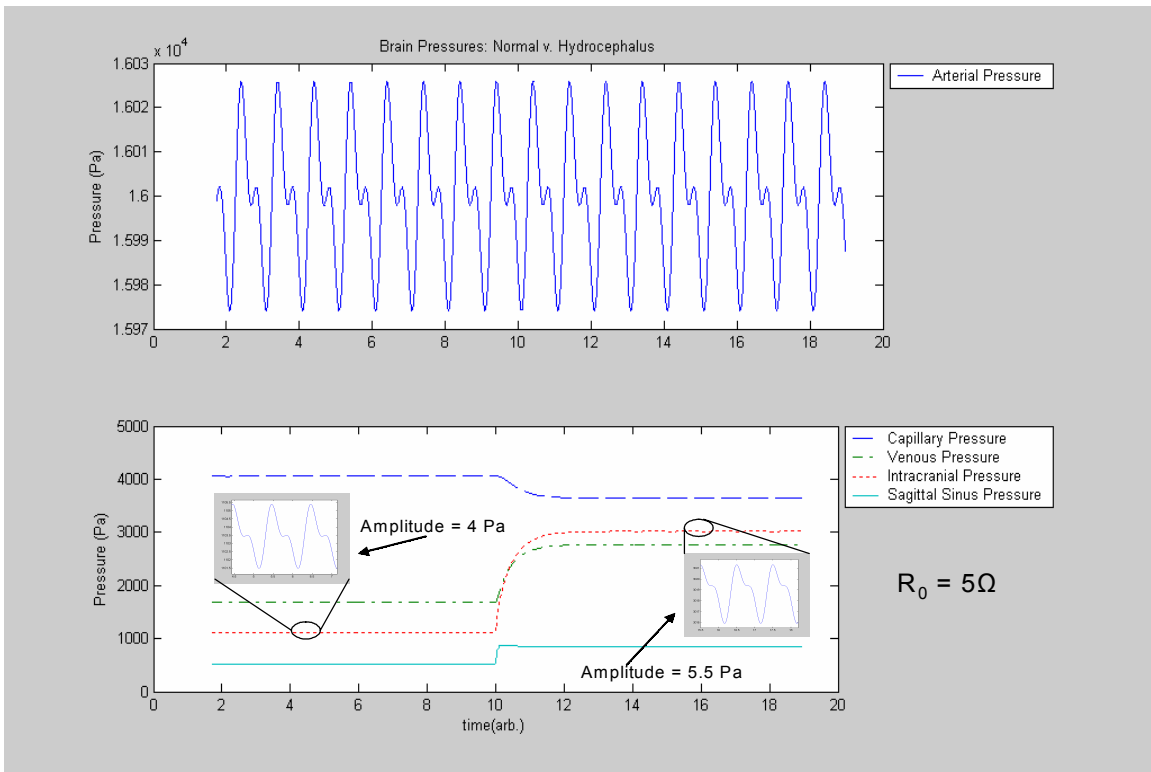


**Figure 6: Simulation run at even lower resistance. Now, capillary pressure is well above ICP.**

### *Compartmental Model: Volumes*

The ICP controls the volume changes in the different compartments of the brain (Ursino 1988). Its relation with the other pressures forms the basis of the volume equations, (3)-(6). Under normal and hydrocephalus conditions in the first simulation, the volume changes are depicted in Figure 7. Following the Monro-Kellie doctrine, the addition of the volume changes in all the compartments equals zero (Winston 1991, Ursino 1998). The venous volume changes more, relative to the arterial volume. This follows physiological data since 70% of the blood is in the venous system, and 25% is in the arterial system, with the other 5% in the capillaries (Danzinger 2003). The changes in tissue, arterial, and venous volumes offset the CSF-Ventricular system volume.

In Figure 7, the volume changes in each of the compartments of the model are shown. The first steady state is normal conditions. The values of the volumes follow physiological data (Ursino 1988, Linninger 2004). With a step change from normal to hydrocephalus, the new steady state shows the new volumes. As can be seen, the ventricular system expands while the other systems contract. This is consistent with experimental and physiological data concerning patients with hydrocephalus (Linninger 2004). Their ventricular system is flooded with CSF and their brain parenchyma is then reduced in size. A further discussion of this is contained later in this document.

During the second simulation (Figure 8), the arterial and brain parenchyma departments change about the same as in the first simulation. However, the venous volume changes less. Therefore, the ventricular system increases less.

In the last simulation (Figure 9), the trend from the second simulation continues. The arterial and brain parenchyma volume change about the same. The venous volume decreases less. This results in a smaller increase in the ventricular system. As the absorption resistances are decreased, hydrocephalus becomes mild. Subsequently, the adverse effects of the disease become less pronounced in each simulation.

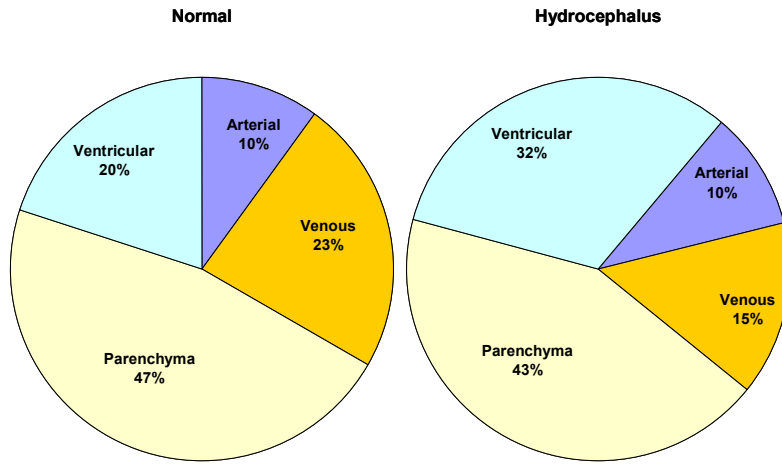
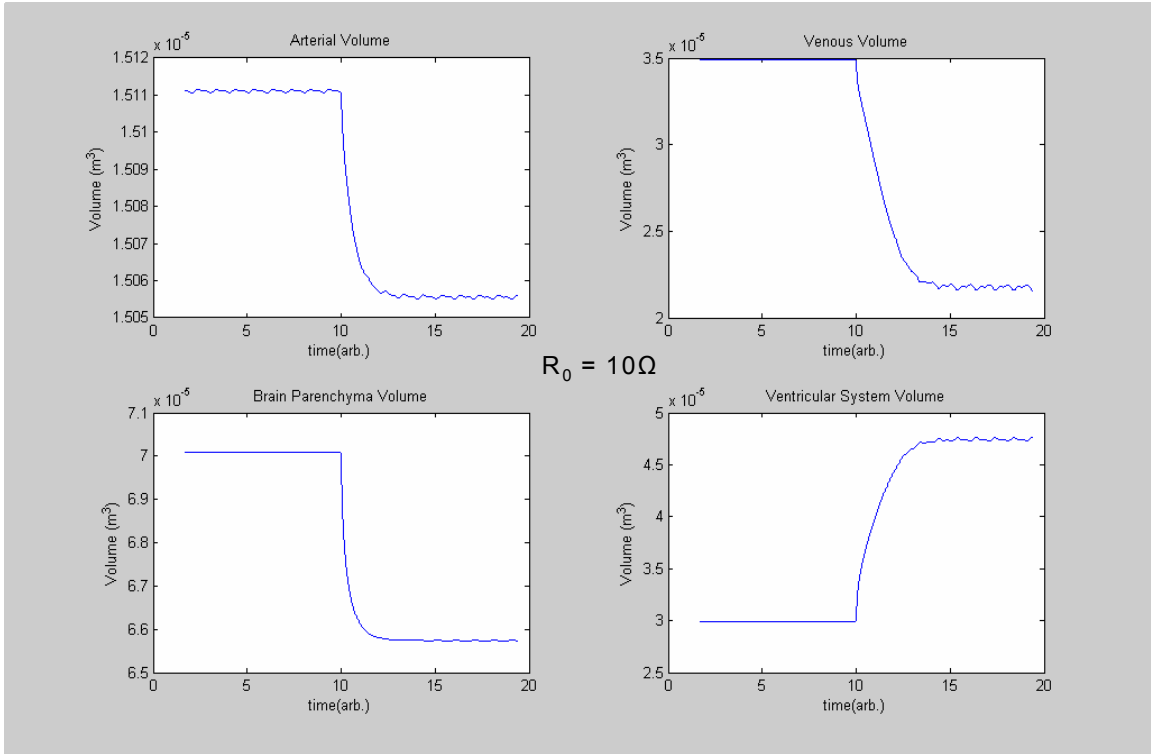


**Figure 7: Volume changes in the compartmental model under normal and hydrocephalus conditions in first simulation.**

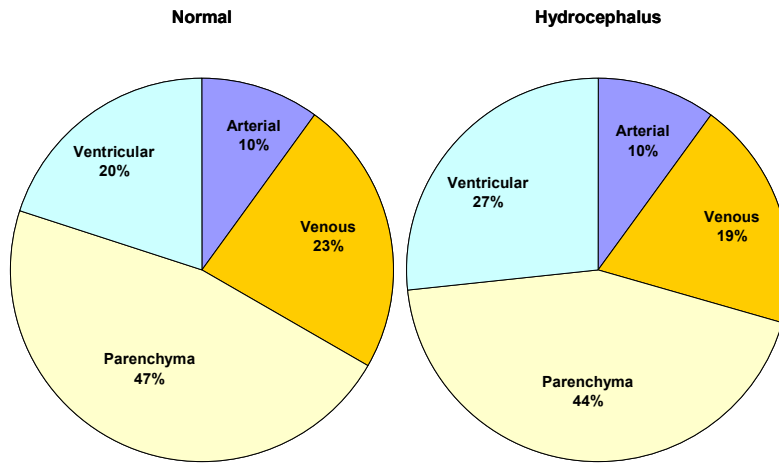
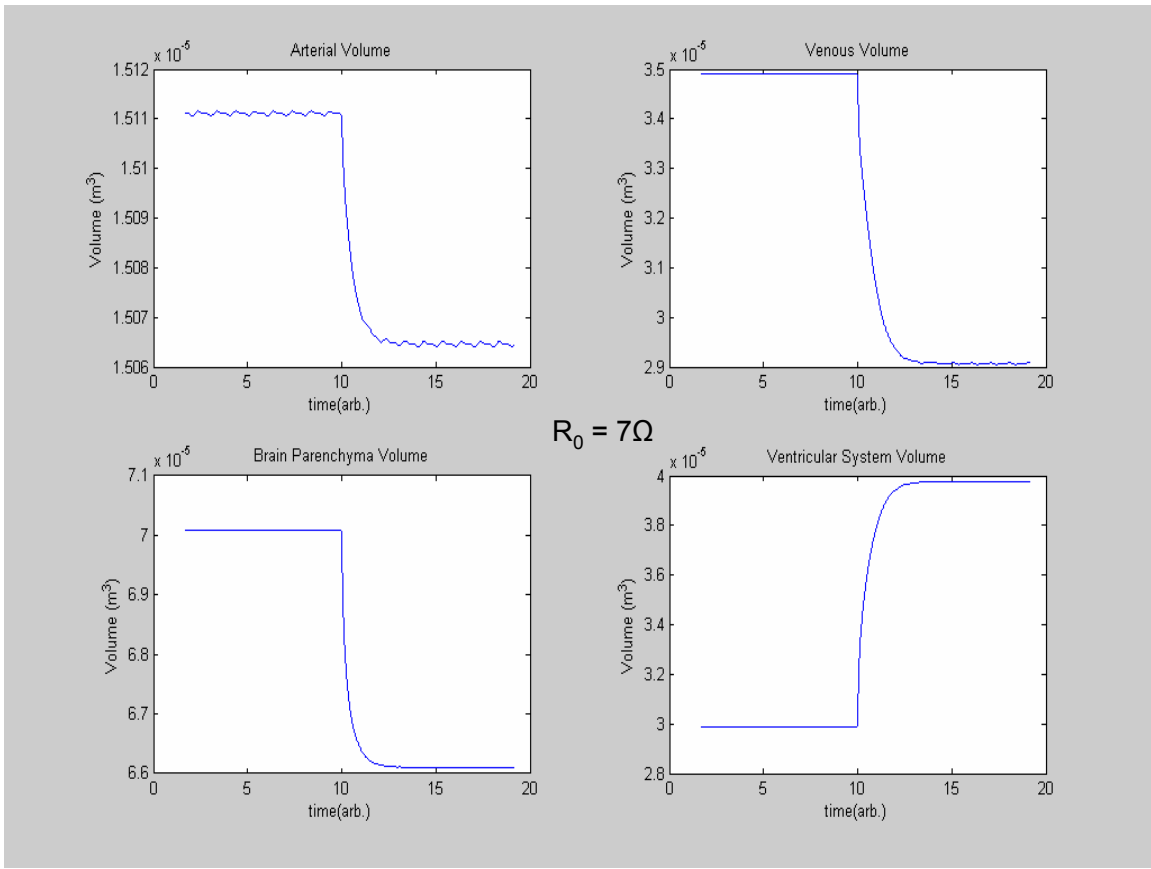


**Figure 8: Volume changes in second simulation.**

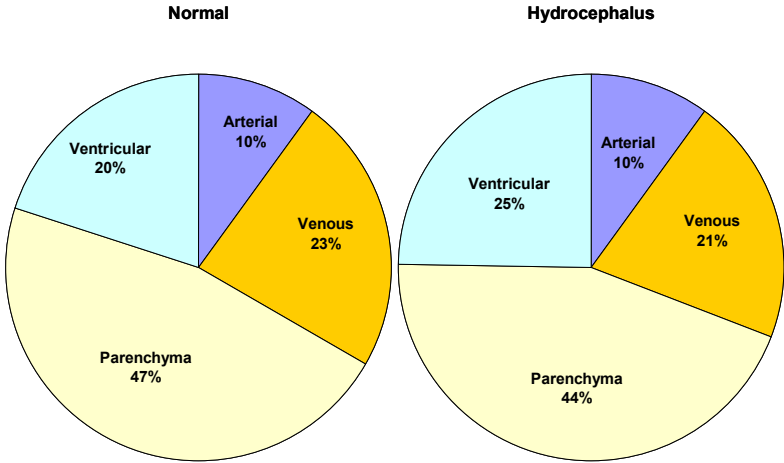
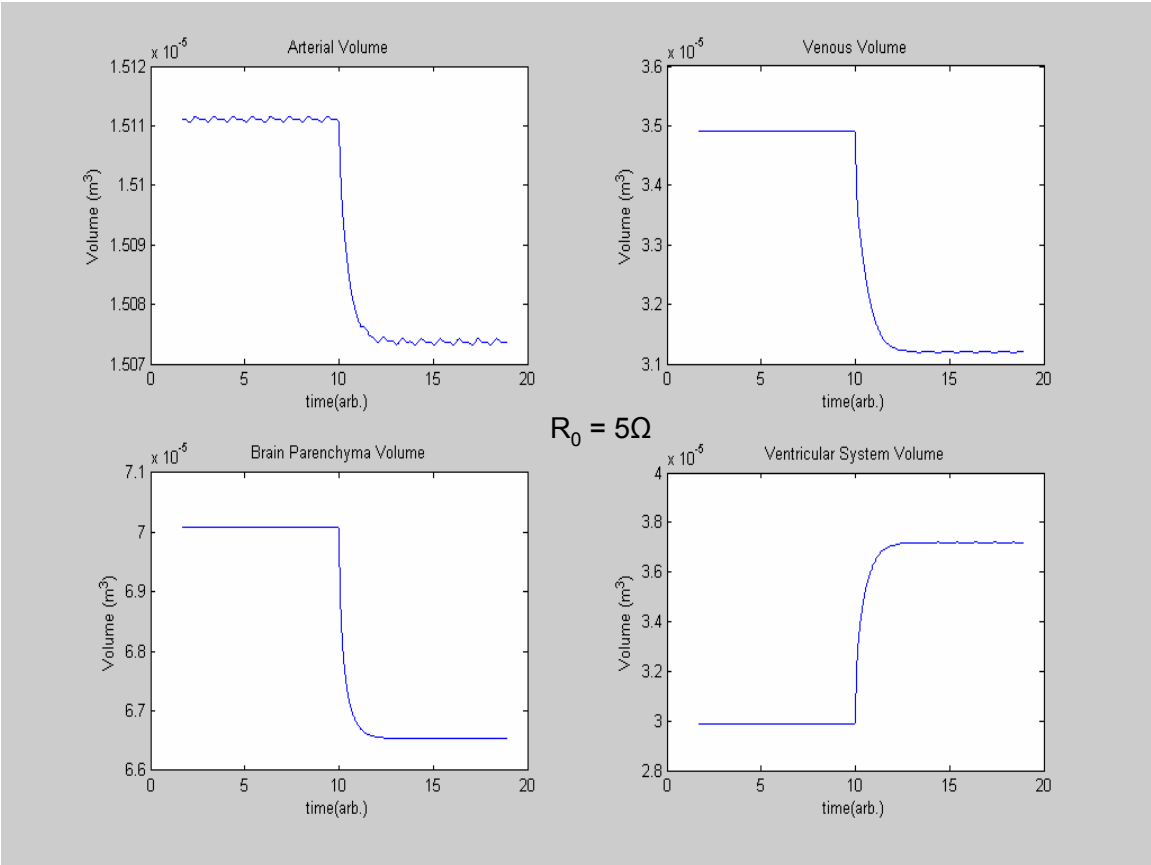
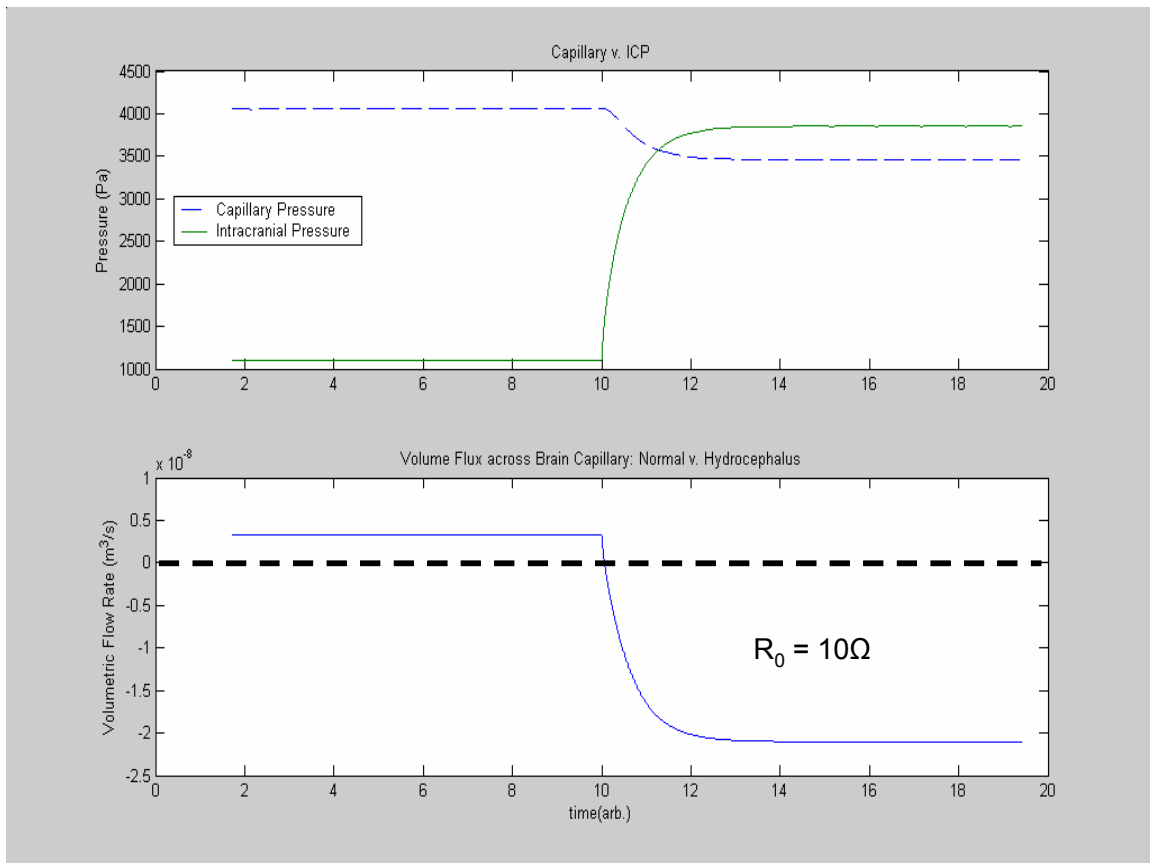


Figure 9: Volume changes in third simulation.

## Cerebral Capillary Fluid Exchange Model

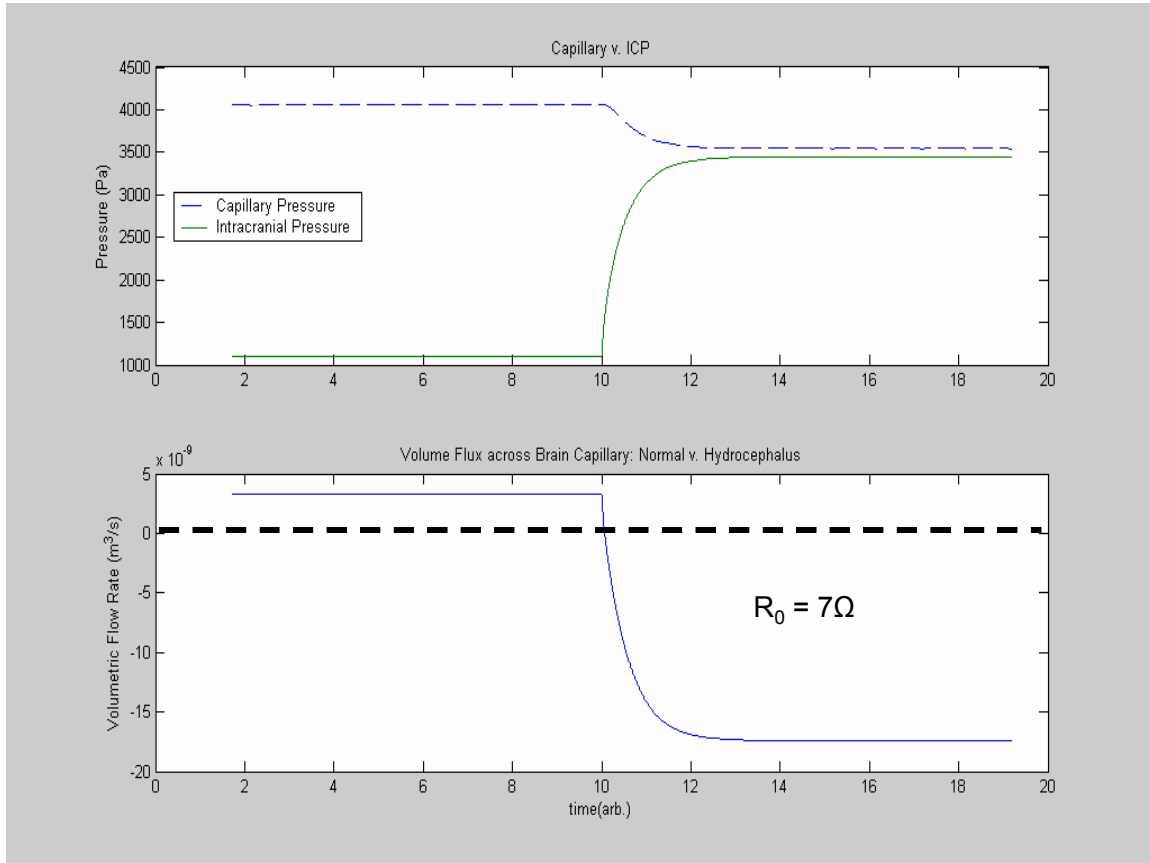
The cerebral capillaries normally supply fluid to the brain parenchyma tissue. The normal flux pattern is positive, which means that water is diffusing out of the capillaries and into the tissue (Paulson 1977). A negative volume flux would mean that water is now being absorbed by the capillaries. Obtaining a negative volume flux under the hydrocephalus regime would support our idea that the mechanism of the reduced parenchyma volume follows this pattern. Nevertheless, without a negative volume flux possible, our idea would not work and Winston (1991) would have more support.

Figure 10 shows the volume flux under normal and hydrocephalus conditions in the first simulation. The top graph shows the comparison of capillary pressure to intracranial pressure (ICP). As can be seen, the flux is normally positive, but then becomes negative when hydrocephalus is imposed on the system. This supports our hypothesis. That the capillary pressure decreases and the intracranial pressure increases above the capillary pressure is the reason for this behavior. This reverse directly causes a backward pressure gradient, which then induces this negative flux flow.



**Figure 10: Extracellular fluid or water volume flux changes from normal to hydrocephalus conditions. The dashed line represents the change from fluid flow out to fluid flow in. The top graph compares capillary pressure to ICP over the course of hydrocephalus development.**

In the second simulation, when the capillary pressure is slightly above the ICP, the reverse volume flux still exists (Figure 11). This provides a mechanism for the brain parenchyma to be reduced in size with hydrocephalus. Even before the ICP rises above the capillary pressure, the conditions that facilitate a negative volume flux exist.



**Figure 11: Volume flux in second simulation.**

Finally, in the third simulation, the flux change still occurs despite the capillary pressure being significantly higher than the ICP (Figure 12). Even in mild cases of hydrocephalus, the water transfer can reverse. At the onset of hydrocephalus, when the ICP begins to increase, a reverse pressure gradient is set. From this data, we can infer that a threshold exists for the change in volume flux. When the ICP reaches a certain level relative to the capillary pressure, this negative flux occurs. A further discussion of this idea is left to the next section.

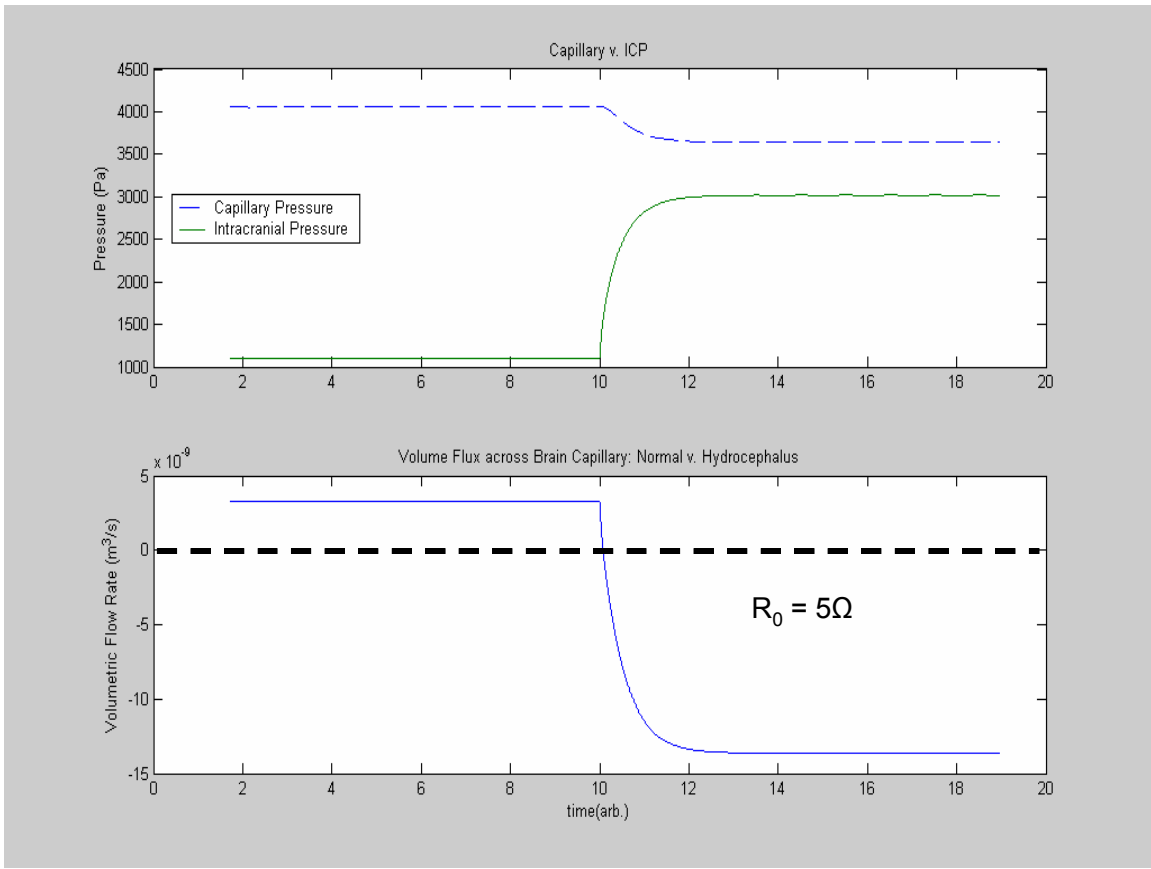


**Figure 12: Volume flux changes in third simulation.**

## Discussion

### *Compartmental Model: Pressures*

The compartmental model represents the pressure and volume dynamics in the brain. At this point, the model is dependent on a circuit analogy of the brain system (Ursino 1988). In this circuit analogy, the pressures are tuned to physiological significance and then plugged into volume equations to obtain the volumes of the different compartments. Therefore, in this model, there exists no feedback from the volume to the pressure. The only relationship is from the pressure to the volume. This is a simple model in comparison to the actual system. However, it follows past experiments and physiological data well (Linninger 2004). While it does not account for the influence of the volume on the pressure, it still predicts pressure and volume changes well.

Looking closely at the pressure waves, it was determined that the amplitude of the oscillations in the arterial, capillary, venous pressure waveforms remain constant. Meanwhile, the oscillation amplitudes in the ICP and Sagittal Sinus pressures increase. These relationships are physiologically consistent (Linninger 2004). An in depth look at the circuit may explain this behavior. Using current and voltage balance laws (Richardson 1990), an attempt was made to develop the pressure (voltage) equations comprising the overall ordinary differential equation system governing the circuit. While some equations were developed, none were successful in simulation. Nevertheless, the equations did further explain the behavior of the oscillation amplitudes. For the equations describing the blood pressures—arterial, capillary, and venous—the resistance term relating to hydrocephalus was not found. Thus, the oscillation amplitudes did not change when hydrocephalus was imposed on the system. In the equations where the amplitudes did increase with hydrocephalus (i.e. CSF pressures)—intracranial and Sagittal Sinus—the resistance term describing hydrocephalus was found (Appendix D).

Moreover, another attempt was made to normalize the resistance and capacitor terms to physiological values. Nevertheless, with the failure of the pressure equations, this was not successful either. These values remained as tuning parameters to obtain physiologically correct pressure waves to be evaluated in the volume and capillary relations.

### *Compartmental Model: Volumes*

The three different simulations were run to track the change in ICP and study the behavior of the volume changes at each point to better understand the system. In the first simulation, when the ICP is above the capillary pressure, the volume changes are most significant. During the second simulation, when capillary pressure is slightly above the ICP, the arterial and brain parenchyma volume changes remain the same. The change in the ventricular volume from the first to second simulations is attributed to the change in the venous volume from simulation to simulation. Since the absorption resistance controls the absorption of the CSF into the venous compartment, the venous volume changes make sense. When the resistance is high, not as much CSF is absorbed. Therefore, not as much mass is transferred from the ventricular system volume to the

venous volume. Instead, the mass stays in the ventricular system and out of the venous volume. When the resistance is relaxed, more CSF is absorbed. This subsequently adds mass to the venous volume. Thus, the venous volume does not decrease as much, and the ventricular system does not increase as much when the absorption resistance is lowered.

The constant  $P_{v1}$  value that is run in the simulation differs from the literature value. The simulation  $P_{v1}$  is nearly one and one-half times the literature value because of mathematical problems encountered in the simulation. The literature value  $P_{v1}$  led to imaginary numbers because the log term of equation (13) became negative during the hydrocephalus regime. To compensate, the  $P_{v1}$  simulation value was adjusted.

The arterial volume does not change significantly. This makes physiological sense. The arterial volume is least affected by the symptoms of hydrocephalus. It remains relatively constant because the blood supply to the brain remains uninterrupted during the disease. Similar to how the arterial pressure wave is unaffected; the arterial volume only decreases minimally.

The parenchyma volume decreases from about 70 cc to 65 cc. This follows the trend in hydrocephalus. The brain tissue is compressed and this is where most of the damage of the disease occurs. As the ventricles expand, the brain tissue contracts. The mechanism of this phenomenon has been the goal of our study. While Winston has claimed that the extracellular fluid drains into the ventricular system, we claim that it is absorbed by the cerebral capillaries and taken away. The volume changes support our hypothesis. In these simulations the brain tissue volume loses about 5 cc of space. Meanwhile, the ventricular system, depending on the resistance value, gains the 5 cc of space plus the CSF that would normally drain in to the venous compartment. The ventricular system does not gain volume from the extracellular fluid. Instead, the extracellular fluid is reabsorbed in to the cerebral capillaries and carried away.

### *Cerebral Capillary Fluid Exchange Model*

To further analyze the system, a model was developed to describe the volume flux changes of water across the cerebral capillaries. Our goal was to determine whether a mechanism exists in which the water can be driven in the reverse direction. From this analysis, it has been determined that at a certain threshold, the pressure gradient does reverse and can pull extracellular fluid into the cerebral capillaries.

Based on equation (18), a threshold can be analyzed and a relationship developed. When the difference between the capillary pressure and the ICP is greater than the change in osmotic pressure, normal conditions exist. Water flows from the capillary and in to the surrounding tissue space. However, when the difference between the capillary pressure and the ICP is less than the change in osmotic pressure, hydrocephalus develops. This means that the ICP does not necessarily need to be greater than the capillary pressure, it needs only to cross this threshold and reverse flow. Hydrocephalus is synonymous with a rise in ICP (Hakim 1976). When the ICP rises and crosses this threshold, a mechanism then exists for the extracellular fluid (or water) to be absorbed by the cerebral capillaries.

The change in the flux from normal conditions to hydrocephalus conditions is depicted conceptually in Figure 13 below.

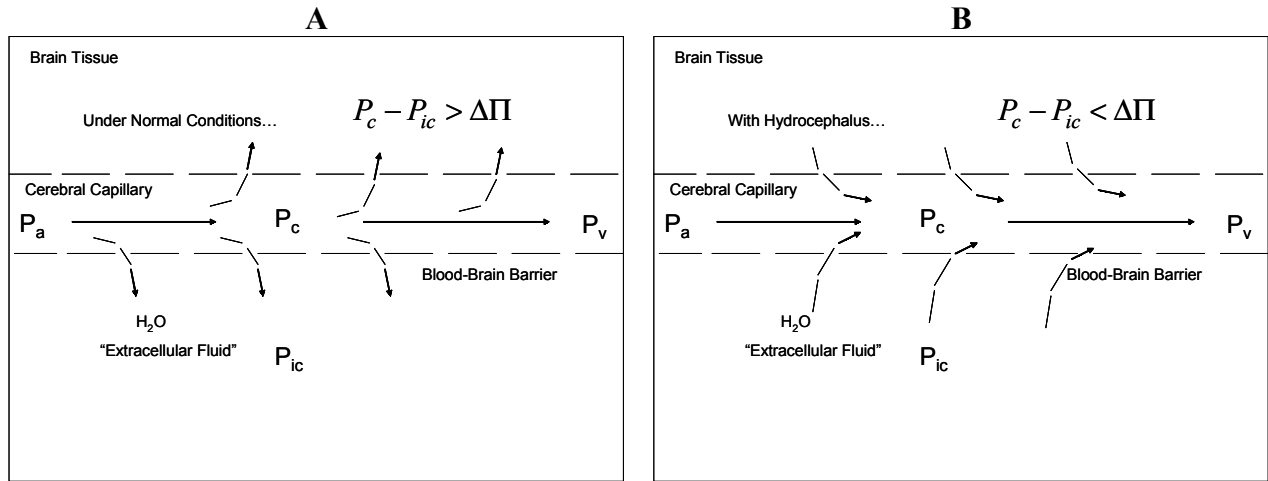


**Figure 13: Conceptual view of change in volume flux of "extracellular fluid" (i.e. water) in the cerebral capillaries.**

## **Conclusion**

The goal of this work was to determine whether a mechanism for reverse extracellular volume flux across a cerebral capillary exists. In this respect, the project was successful and a mechanism is described. While solving this problem, a compartmental model describing the pressure-volume dynamics was established. In this model, a circuit was analyzed and the voltages were found. The voltages in the circuit analogy represent the brain pressures. These pressures were then used to determine the brain compartment volumes. The volume changes followed our expectations and those found in previous work (Linninger 2004).

From this circuit and the forthwith pressures, the mechanism for reverse extracellular volume flux across the cerebral capillary membrane was found. Future work from this finding would entail further analysis of the cerebral capillaries. This would include simulations in more complex programs such as FLUENT and Gambit to find the pressure flow fields, and eventually, the mass transfer. Furthermore, modeling the fluid exchange to the molecular level would prove beneficial. Currently, the model is macroscopic and a generalization. A more detailed approach is necessary.

Future work on the compartmental model includes a manual circuit analysis to decipher the circuit and to determine the pressure equations rather than simply running a simulation. Obtaining the pressure equations will allow us to understand the intricacies of the model and be able to fully evaluate it. While an attempt was made to complete this proposal during the summer, time constraints, ultimately, led to this failure.

### **Acknowledgements**

Prof. A. Linninger  
Michalis Xenos, Post Doc  
Andres Malcom, Grad Student  
National Science Foundation

## References

Danzinger, Z.; Linninger, A. Modeling cerebral blood flow and pressure in elastic tubes using a finite element approach: its relation to symptoms in hydrocephalus. LPPD Report, <http://vienna.che.uic.edu/Laboratory/laboratory.htm>, 2003.

Fournier, R.L. Basic Transport Phenomena in Biomedical Engineering. Taylor & Francis, Inc., 1998.

Hakim, S.; Venegas, J.G.; Burton, J.D. The physics of the cranial cavity, hydrocephalus and normal pressure hydrocephalus: mechanical interpretation and mathematical model. *Surg. Neurol.* 5: 187-210, 1976.

Linninger, A.A.; Tsakiris, C.; Zhu, D.C.; Penn, R. Pulsatile cerebrospinal fluid dynamics in the human brain. LPPD Report, <http://vienna.che.uic.edu/Laboratory/laboratory.htm>, 2004.

MacLeod, R. Microcirculation. BioEngineering 6000: Systems Physiology Lecture, <http://www.cvrti.utah.edu/~macleod/be6000/notes/L23-Microcirculation-bw.pdf>, 2004.

Paulson, O.B.; Hertz, M. M.; Bolwig, T.G.; Lassen, N.A. Filtration and diffusion of water across the blood-brain barrier in man. *Microvasc. Res.* 13:113-124, 1977.

Richardson, J.; Reader, G. *Electrical Circuit Analysis*. Ellis Horwood Limited, 1990.

Roycewicz, P. Internal volume measurement sensor for use in the CSF ventricular system. LPPD Report, <http://vienna.che.uic.edu/Laboratory/laboratory.htm>, 2004.

Ursino, M. A mathematical study of human intracranial hydrodynamics. 1. The cerebrospinal fluid pulse pressure. *Ann. Biomed. Eng.* 16: 379-402, 1988.

Ursino, M.; Di Giammarco, P. A mathematical model of the relationship between cerebral blood volume and intracranial pressure changes: the generation of plateau waves. *Ann. Biomed. Eng.* 19: 15-42, 1991.

Ursino, M.; Lodi, C.A. A simple mathematical model of the interaction between intracranial pressure and cerebral hemodynamics. *J. Appl. Physiol.* 82: 156-1269, 1997.

Winston, K.R.; Breeze, R.E. Hydraulic regulation of brain parenchymal volume. *Neurol. Res.* 13: 237-247, 1991.

Xenos, M. *Palse.nb*. Mathematica file. LPPD, 2004.

Zagzoule, M. Marc-Vergnes, J.P. A global mathematical model of the cerebral circulation in man. *J. Biomechanics* 19(12): 1015-1022, 1986.



## Appendix B

**function pressures**

**clear workspace;**

**%Import pressure waveform data from Simulink and PLECS  
load pressures;**

**%Initialize time and pressures**

**t=Pa(8000:32000,1);  
Pa=Pa(8000:32000,2);  
Pc=Pc(8000:32000,2);  
Pv=Pv(8000:32000,2);  
Pic=Pic(8000:32000,2);  
Pvs=Pvs(8000:32000,2);**

**%Plot pressures**

**figure(1);  
subplot(2,1,1),plot(t,Pa)  
title('Brain Pressures: Normal v. Hydrocephalus')  
ylabel('Pressure (Pa)')  
legend('Arterial Pressure',-1)  
subplot(2,1,2),plot(t,Pc,'--',t,Pv,'-.',t,Pic,':',t,Pvs)  
legend('Capillary Pressure','Venous Pressure','Intracranial Pressure','Sagittal  
Sinus Pressure',-1);  
xlabel('time(arb.)')  
ylabel('Pressure (Pa)')**

**%Arterial Volume**

**Ka=3.68e6; %Arterial constant  
Va=log(Pa-Pic)/Ka+1.25e-5;**

**figure(2)**

**subplot(2,2,1),plot(t,Va)  
title('Arterial Volume')  
xlabel('time(arb.)')  
ylabel('Volume (m^3)')**

**%Venous Volume**

**Kv=3.1e5; %Venous constant  
Pv1=-633; %Transmural pressure at which cerebral veins collapse  
Vv=log(Pv-Pic-Pv1)/Kv+1.2e-5;**

**subplot(2,2,2),plot(t,Vv)**

```

title('Venous Volume')
xlabel('time(arb.)')
ylabel('Volume (m^3)')

%Brain Parenchyma Volume
Ke=2.6e5;    %Brain parenchyma constant
P01=1000;   %Constant pressure parameter
Vtiss=-((P01^2)/Ke)*(log((Pic).^2 + (P01^2)*Pic)./(2*Pic + (P01^2)))+15e-5;

subplot(2,2,3),plot(t,Vtiss)
title('Brain Parenchyma Volume')
xlabel('time(arb.)')
ylabel('Volume (m^3)')

%Ventricular System Volume
Vcsf=-(Vtiss-7e-5)-(Va-1.5e-5)-(Vv-3.5e-5)+3e-5;

subplot(2,2,4),plot(t,Vcsf)
title('Ventricular System Volume')
xlabel('time(arb.)')
ylabel('Volume (m^3)')

%Constants in volume flux equation
LpS=7.26e-12; %hydraulic conductance * surface area of capillaries
piC=3300;    %capillary osmotic pressure
piICP=800;   %intracranial osmotic pressure

%Volume flux of water across brain capillary
J=LpS*((Pc-Pic)-(piC-piICP));

figure(4)
subplot(2,1,2), plot(t,J)
title('Volume Flux across Brain Capillary: Normal v. Hydrocephalus')
xlabel('time(arb.)')
ylabel('Volumetric Flow Rate (m^3/s)')

subplot(2,1,1), plot(t,Pc,'--',t,Pic)
legend('Capillary Pressure','Intracranial Pressure',0)
title('Capillary v. ICP')
ylabel('Pressure (Pa)')figure(4)

```

## Appendix C

**Table 1: Properties used in simulations compared to literature**

<u>Property</u>	<u>Value</u>	<u>Literature Value</u>	<u>Reference</u>
$R_4^*$	6 $\Omega$	N/A (used to tune pressure waveform)	-----
$R_1^*$	2.5 $\Omega$	N/A (used to tune pressure waveform)	-----
$R_3^*$	3.25 $\Omega$	1.24 mmHg·s·ml <sup>-1</sup>	Ursino 1997
$R_5^*$	1 $\Omega$	N/A (used to tune pressure waveform)	-----
$R_f^*$	1 $\Omega$	2.38×10 <sup>3</sup> mmHg·s·ml <sup>-1</sup>	Ursino 1997
$R_0^*$	1 $\Omega$ -5 $\Omega$ -7 $\Omega$ -10 $\Omega$	526.3 mmHg·s·ml <sup>-1</sup>	Ursino 1997
$C_{ai}^*$	100×10 <sup>-3</sup> F	0.15 ml/mmHg	Ursino 1997
$C_{vi}^*$	100×10 <sup>-3</sup> F	0.46 cm <sup>3</sup> /mmHg	Ursino 1988
$C_{tiss}^*$	100×10 <sup>-3</sup> F	0.30 cm <sup>3</sup> /mmHg	Ursino 1988
$K_a$	3.68×10 <sup>6</sup> m <sup>-3</sup>	3.68 cm <sup>-3</sup>	Ursino 1988
$K_v$	3.1×10 <sup>5</sup> m <sup>-3</sup>	0.31 cm <sup>-3</sup>	Ursino 1988
$K_E$	2.6×10 <sup>5</sup> m <sup>-3</sup>	0.26 cm <sup>-3</sup>	Ursino 1988
$P_{v1}^+$	-633 Pa	-2.5 mmHg	Ursino 1988
$P_{01}$	1000 Pa	7.5 mmHg	Ursino 1988
$V_{ai}$	15 cm <sup>3</sup>	~20% of 52.5 mL (blood volume)	Ursino 1997 Danzinger 2003
$V_{vi}$	35 cm <sup>3</sup>	~75% of 52.5 mL (blood volume)	Ursino 1997 Danzinger 2003
$V_{tissi}$	70 cm <sup>3</sup>	~5% of 52.5 mL (blood volume) deduced from ~150 cm <sup>3</sup> (total cranium volume)	Ursino 1997 Danzinger 2003 Linninger 2004
$V_{CSFi}$	30 cm <sup>3</sup>	30 cm <sup>3</sup>	Linninger 2004
$L_p \cdot S$	7.26×10 <sup>-12</sup> m <sup>3</sup> /Pa·s	7.26×10 <sup>-12</sup> m <sup>3</sup> /Pa·s	Paulson 1977
$\Pi_c$	3300 Pa	28 mmHg	MacLeod 2004
$\Pi_{ic}$	800 Pa	6 mmHg	MacLeod 2004

\* - not physiologically significant value; used only to tune voltage waves in circuit to form physiologically significant brain pressure waveforms.

+ - value adjusted because of mathematical problems in hydrocephalus regime during simulation.

## Appendix D

Here are the pressure equations developed by implementing current and voltage balances across the circuit analogy (Richardson 1990). While these equations failed in the MATLAB simulation, they still give insight into the behavior of the oscillation amplitudes.

$$P_a = 17.5 \sin(2\pi t - \frac{\pi}{2}) - 12.5 \sin(4\pi t) + 16000 \quad (19)$$

$$P_c = \frac{1}{\delta_c} [\delta_f (P_v - P_{ic} + P_{vs}) + \delta_v P_v] \quad (20)$$

$$\frac{dP_v}{dt} = \frac{\frac{1}{K_a (P_a - P_{ic})} [\delta_a P_a - \delta_v P_v - \delta_f (P_v - P_{ic} + P_{vs})] + \left(1 + \frac{\delta_f}{\delta_v}\right) \left[ \frac{1}{K_v (P_v - P_{ic} - P_{v1})} (\delta_{vs} P_{vs} - \delta_v P_v) \right]}{1 + \frac{\delta_f}{\delta_c} + \frac{\delta_v}{\delta_c}} \quad (21)$$

$$\frac{dP_{vs}}{dt} = \frac{1}{K_E \left[ P_{ic} + \left( \frac{P_{ic}}{P_{01}} \right)^2 \right]} (\delta_a P_a - \delta_0 P_{ic} - \delta_{vs} P_{vs}) - \frac{1}{K_v (P_v - P_{ic} - P_{v1})} (\delta_{vs} P_{vs} - \delta_v P_v) \quad (22)$$

$$\frac{dP_{ic}}{dt} = \frac{1}{K_E \left[ P_{ic} + \left( \frac{P_{ic}}{P_{01}} \right)^2 \right]} (\delta_a P_a - \delta_0 P_{ic} - \delta_{vs} P_{vs}) \quad (23)$$

The mass transfer rate,  $\delta$ , is equivalent to  $1/R$  in circuit terms. Note the appearance of the Sagittal Sinus mass transfer rate,  $\delta_0$ , in the CSF pressure equations, (22)-(23), but not the blood pressure equations, (19)-(21). This is the mass transfer rate that is manipulated to simulate the conditions of hydrocephalus.